Shubnikov–de Haas Effect in Bismuth. II

LAWRENCE S. LERNER
Hughes Research Laboratories, Malibu, California
(Received 14 December 1962)

We have measured the oscillatory component of the transverse magnetoresistance of bismuth as a function of magnetic field orientation at 1.2°K. We have observed spin splitting of the first few Landau levels for magnetic field along both the binary and bisectrix axes. The Shubnikov–de Haas periods indicate a marked deviation of the light-electron Fermi surface from ellipsoidal form, for magnetic field orientations near the binary axis; we compare our results with the Cohen nonellipsoidal model. We observe the light-hole Fermi surface throughout the range of orientation. By comparison with earlier results, we establish that the previously observed heavy carriers are electrons. We observe a new fourth set of periods, which we attribute to a heavy-hole Fermi surface of trefolioid form; the square of the mean Fermi momentum is $m_0\kappa_H^2 \approx 3.8\, m_0$ milli-electron volts.

I. INTRODUCTION

IN an earlier paper[1] (which we will call paper I) we reported on measurements of the Shubnikov–de Haas effect in bismuth. A sensitive differential technique was used to observe the quantum oscillations in the magnetoresistance at liquid-helium temperatures. On the basis of these results and those of other experiments, we proposed two possible three-carrier models and a possible four-carrier model of the Fermi surface of bismuth.

We have repeated these observations on a different set of bismuth samples. It is the principal purpose of this paper to bring this new experimental evidence to bear upon the problem of the Fermi surface of bismuth.

II. EXPERIMENTAL

The apparatus employed was in all respects identical to that described in paper I, except that a different X–Y recorder was used. The samples used were prepared by Zitter, who has described the process elsewhere.[2] Table I compares the history of Bi Ia, Ib, and II (the samples described in paper I) with that of Bi III and IV (Zitter's samples).

The measurements were made at 1.2°K; the magnetic field orientations covered in detail one sextant of the X–Y plane (Bi III) and one quadrant of the Y–Z plane (Bi IV). In addition, measurements were made at a few other widely distributed orientations in order to check the expected symmetry, and hence the alignment of the samples in the apparatus.

III. RESULTS AND ANALYSIS

General

The data obtained are similar in general character and appearance to those discussed in paper I. An important difference, however, is that the new data yield considerably more information about short periods (down to approximately 0.1×10^{-5} G^{-1}) than did the data of paper I (where no periods shorter than 0.5×10^{-5} G^{-1} were observed). At the same time, the multitude of short periods tends to obscure the long periods, so that less information is available about the latter than was the case in the work reported in paper I. This difference is exemplified by the data shown in Fig. 1, obtained from Bi III with $H \parallel$ binary axis. Comparison should be made with Fig. 8(a) of paper I, which was obtained from Bi Ib at the same field orientation and at the same temperature. What appeared to be noise in the earlier experiment is resolved into very distinct oscillations in the new experiment. The small bump at $H \approx 13.8$ kG in Fig. 8(a) of paper I is now observed clearly enough (arrows in Fig. 1) to be attributed with some confidence to spin splitting. We will discuss this point in more detail below. It is reasonable to attribute the improvement in resolution to the fact that Bi III and Bi IV were grown

TABLE I. Comparison of bismuth samples.

Samples	Source	Nominal as-received purity	Preparation	Cutting	Approx. dimensions (cm)	Final purity
Ia, Ib, II	Cerro de Pasco	99.998%	Zone-refined in vacuo	Toothless band saw with SiC-glycerine-water slurry	0.15×0.2×1.5	99.9999% by spectrography and neutron activation
III, IV	Canadian Mining and Smelting Co., Ltd.	99.9999% (zone refined)	Bridgman technique under DC704 silicone oil	Spark cutter	0.8×0.8×6	Not measured

[1] L. S. Lerner, Phys. Rev. **127**, 1480 (1962).
[2] R. N. Zitter, Phys. Rev. **127**, 1471 (1962).

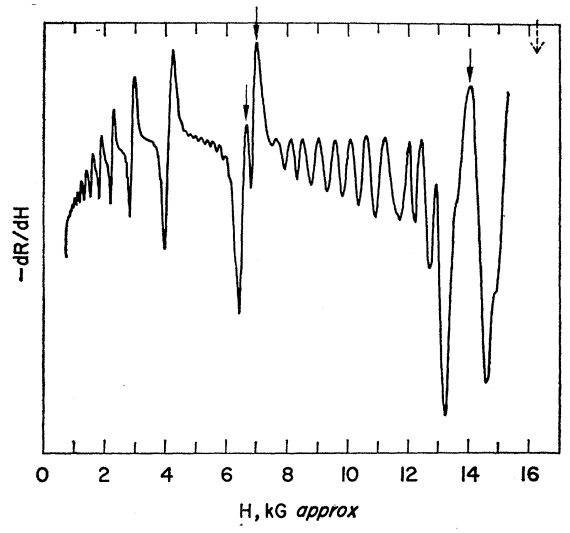

FIG. 1. Differential Shubnikov–de Haas oscillations for $\psi = -30°$. The solid arrows locate the spin-split peaks; the dashed arrow indicates the approximate expected H value of the highest field spin-split peak, which lies beyond the maximum field attainable by our magnet.

more slowly than Bi Ia, Ib, and II, and cut by the very gentle spark erosion technique. They may therefore be presumed to possess a higher degree of crystal perfection.

IV. DISCUSSION

Spin Splitting

Boyle *et al.*[3] have observed spin splitting in the magnetothermal oscillations in bismuth, with the magnetic field parallel or nearly parallel to the binary axis. As noted above, we have observed this splitting clearly in the oscillations attributable to the first and second quantum levels of the light electrons.[4] In the original data, a slight jog is barely detectable in third oscillation (at $H \approx 4$ kG), but this detail is lost in the reproduction and reduction involved in the preparation of Fig. 1. We could not quite reach the magnetic field necessary to see the higher of the first pair of peaks; the estimated position of this peak is indicated by a dashed arrow.

The splitting is also clearly visible for $H \parallel$ bisectrix axis (Fig. 2). Here the Shubnikov–de Haas period is somewhat longer than for $H \parallel$ binary, and the complete set of light-electron oscillations is visible in the magnetic field range available to us.

The spin splitting presumably is also present between the binary and bisectrix axes, but it is impossible to identify it as such because of the complicated background of oscillations in the nonprincipal directions.

We may use our data to calculate the splitting parameter Δ.[3,5] The value obtained from two binary orientations (that depicted in Fig. 1 and one other orientation) is $\Delta = 0.46_5 \pm 0.01$, and the value from two bisectrix orientations (that depicted in Fig. 2 and one other) is $\Delta = 0.48_5 \pm 0.01$. The binary value agrees with that of Boyle *et al.* The discrepancy between the Δ's for the binary and bisectrix orientations is unexpected on the basis of the theory of Cohen and Blount.[5]

The spin splitting does not appear in those few orientations (e.g., $\phi = 45°$) where there is a relatively short light-electron period almost unaccompanied by beats. In these situations, however, we are observing oscillations of high ordinal number; the levels in which we have observed splitting have all been of low ordinal number. Likewise, no spin splitting appears in the orientations near the trigonal axis ($\phi = 90°$), where the light holes dominate.

The Light-Electron Fermi Surface

The Shubnikov–de Haas periods extracted from the data are plotted in Fig. 3. In interpreting these data we adopt the procedure of first fitting groups of periods to previously observed pieces of Fermi surface, and comparing the results with those of earlier work. We then turn our attention to the remaining periods. Finally, we discuss the complete Fermi surface.

We attribute the periods denoted as circles in Fig. 3 to the light-electron surfaces.[1] The principal difference between these data and earlier results on the light-electron periods is the relative dominance here of the short periods. In particular, we have, apparently for the first time, traced the principal light-electron periods all the way to the trigonal and binary axes.

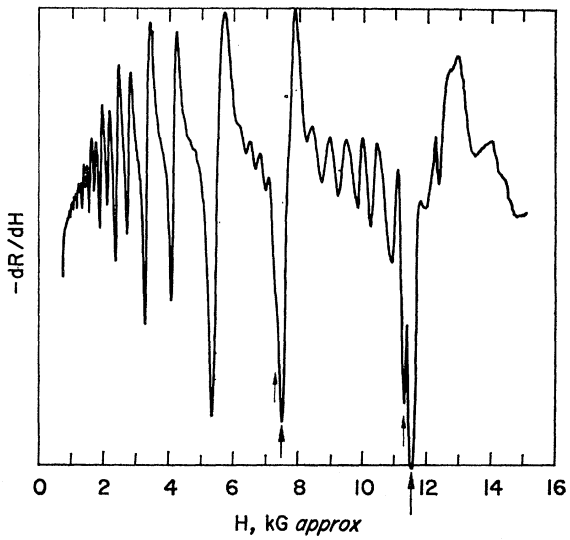

FIG. 2. Differential Shubnikov–de Haas oscillation for $\psi = 0°$. The arrows locate the spin-split peaks.

[3] W. S. Boyle, F. S. L. Hsu, and J. E. Kunzler, Phys. Rev. Letters **4**, 278 (1960).

[4] The ordinal number one is assigned to the highest field (lowest $1/H$) oscillation.

[5] For a discussion of the theory of the spin splitting of quantum oscillation levels, see M. H. Cohen and E. I. Blount, Phil. Mag. **5**, 115 (1960).

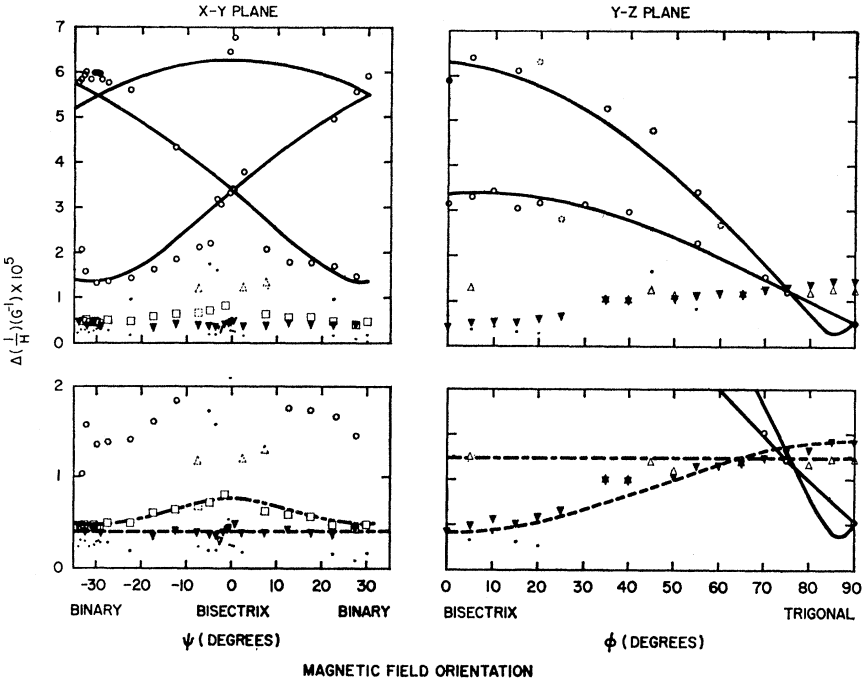

FIG. 3. Shubnikov–de Haas periods as a function of magnetic field orientation. The lower plots repeat some of the data of the upper plots on an expanded scale. Solid curves are a fit of the ellipsoid model for the light electrons. The dashed curve traces the light-hole ellipsoid. The dash-dot line traces the heavy-electron sphere in the Y–Z plane. The dash-dot-dot curve sketches the heavy-hole surface in the X–Y plane. Circles are electron periods, full triangles light-hole periods, open triangles heavy-electron periods, open triangles heavy-electron periods, and squares heavy-hole periods. Small dots are unexplained; most of those at very small ordinate values are probably spurious. Periods whose assignment to a piece of Fermi surface is uncertain are dashed.

We have made the best fit to these periods of the expressions

$$H\perp\text{trigonal }(X\text{–}Y\text{ plane}),$$
$$P_{\psi_1}=(e\hbar/\nu c)(\kappa_1^2\cos^2\psi+\kappa_2^2\sin^2\psi)^{1/2}, \tag{1a}$$

and two similar expressions differing in phase from Eq. (1a) by $\pm60°$, and

$$H\perp\text{binary }(Y-Z\text{ plane})$$
$$P_{\phi_1}=(e\hbar/\nu c)[\kappa_3^2\sin^2\phi+\tfrac{1}{4}(3\kappa_1^2+\kappa_2^2)\cos^2\phi \pm\kappa_4^2\sin\phi\cos\phi]^{1/2}, \tag{1b}$$
$$P_{\phi_2}=\frac{e\hbar}{\nu c}(\kappa_3^2\sin^2\phi+\kappa_2^2\cos^2\phi\mp2\kappa_4^2\sin\phi\cos\phi)^{1/2}, \tag{1c}$$

where[6]

$$\nu^2=\tfrac{1}{4}m_0^2\kappa_1(\kappa_2^2\kappa_3^2-\kappa_4^4). \tag{1d}$$

The notation here is that of Eq. (4) in paper I. The angles ψ and ϕ are both measured from the bisectrix axis. The signs of the last terms in Eqs. (1b) and (1c) depend on the quadrant chosen. For our data, a good fit requires the choice of the upper signs.

In paper I, we were able to achieve a satisfactory fit by adopting Aubrey's values[7] of the effective masses and adjusting ζ_e, the "parabolic" Fermi energy.[8] Here the fit obtained by such a procedure is not good, especially for the short periods which predominate in this work. We have therefore made a trial-and-error adjustment of Eqs. (1a,b,c,d) to the experimental data. As our data give little information as to the tilt angle α,[9] we attempted to adjust the κ_i^2 in such a way as to keep α the same as that given by Aubrey.[7] We also fixed ν at the value determined in paper I. This procedure yields a very poor fit to the data, especially for the long periods. We obtained a good fit by reducing α to approximately 3°. Changing ν does not improve the fit. Fixing ν automatically gives us the same electron concentration as that in paper I, i.e., $n_e=1.01\times10^{17}$ cm^{-3}-ellipsoid^{-1}. The values of the κ_i which we obtain by the procedure are

$$\kappa_1^2=1.38\text{ meV};\quad \kappa_2^2=29.3\text{ meV};$$
$$\kappa_3^2=0.195\text{ meV};\quad \kappa_4^2=-1.68\text{ meV}.$$

Table II compares the ratios κ_1^2/κ_2^2, κ_3^2/κ_2^2, and $-\kappa_4^2/\kappa_2^2$ with those obtained by other investigators.[7,10–15] It is not our principal purpose to add yet another set of anisotropy ratios to those already in the literature. We have already remarked that the presence of many

[6] Note that the definition of ν^2 in reference 1 [Eq. (4d)] is in error by a factor m_0.

[7] J. E. Aubrey, thesis, Cambridge University, Cambridge, England, 1958 (unpublished).

[8] The parameter ζ_e would be equal to the true Fermi energy η if the bands were parabolic; otherwise, ζ_e is related to η by a dimensionless factor. See reference 1.

[9] The fact that the light-electron ellipsoids are tilted slightly out of the X–Y plane gives rise to the parameter κ_4^2 in Eq. (1). The tilt angle is $\alpha=\frac{1}{2}\text{ arc cot}[(\kappa_2^2-\kappa_3^2)\kappa_4^2/\kappa_2^2\kappa_3^2]$.

[10] D. Shoenberg, Proc. Roy. Soc. (London) **A170**, 341 (1939).

[11] D. H. Reneker, Phys. Rev. **115**, 303 (1959).

[12] J. E. Aubrey, J. Phys. Chem. Solids **19**, 321 (1961).

[13] J. K. Galt, W. A. Yager, F. R. Merritt, B. B. Cetlin, and A. D. Brailsford, Phys. Rev. **114**, 1396 (1959).

[14] J. E. Aubrey and R. G. Chambers, J. Phys. Chem. Solids **3**, 128 (1957).

[15] G. E. Smith, Phys. Rev. **115**, 1561 (1959).

TABLE II. Light-electron anisotropy ratios.

	κ_1^2/κ_2^2	κ_3^2/κ_2^2	$-\kappa_4^2/\kappa_2^2$
Shoenberg[a]	0.0006	0.02	0.1
Reneker[b]	0.0027	0.013	0.085
Aubrey[c]	0.0042	0.02	0.1
Aubrey[d]	0.0042	0.02	0.1
Galt *et al.*[e]	0.0049	0.013	0.089
Aubrey and Chambers[f]	0.0060	0.02	0.1
Smith[g]	0.0061	0.019	0.085
Present work	0.047	0.0067	0.057

[a] See reference 10.
[b] See reference 11.
[c] See reference 7.
[d] See reference 12.
[e] See reference 13.
[f] See reference 14.
[g] See reference 15.

short-period oscillations tends to degrade the accuracy of the analysis of long-period oscillations, and our anisotropy ratios are not superior in accuracy to the older results. Moreover, as we have stated in paper I, the long-period Shubnikov–de Haas oscillations observed by us and by others are not exactly periodic in $1/H$, and we cannot in any case place much weight on the numerical values extracted from them.[16] We have taken the trouble to make a good fit in order to compare the ellipsoidal model based upon it (the solid curve in Fig. 3) with the observed periods. There is a marked deviation of the light-electron Fermi surface from the ellipsoidal-model curve within 30° of the principal binary field orientation (i.e., the short periods near the binary axis); this corresponds to a flattening of the tips of the cigar-shaped light-electron Fermi surface from exact ellipsoidal shape. This flattening is in qualitative agreement with Cohen's nonellipsoidal model[17] of the Fermi surface as developed in detail by Weiner.[18] In making the fit of the ellipsoidal curve to the data, we have chosen to force good agreement at and near the principal binary orientation (i.e., the short periods near the binary axis) and to observe the misfit in the region $0°\lesssim|\psi|\lesssim15°$. Since the predicted deviation from ellipsoidal shape is most marked at the principal binary direction, this procedure may appear to be less logical than making a fit in the region $0°\lesssim|\psi|\lesssim15°$, and observing the misfit near the binary. We prefer our procedure nonetheless, as the data are more accurate at the binary axis, and either method will serve to point out the misfit.

We have attempted to make a better fit to the short-period points near the binary axis, using Weiner's Eq. (14) as a correction to the ellipsoidal model. We have also attempted to make a purely empirical correction by adding to Eq. (1a) a term of the form $\lambda\sin^4\psi$, with λ an adjustable coefficient. These attempts have been unsuccessful for reasonable choices of the coefficients κ_i^2 and λ; the departure of the points from an ellipsoidal plot becomes appreciable at orientations too far from the binary axis. It appears, however, that Weiner's estimate of a 15% correction in the short binary period is too small. The results of Brown *et al.*,[19] indicate that the energy gap in Bi is $E_g=15$ meV, or only about one-third as large as the value assumed by Weiner. This leads to a value $\eta=30$ meV. In order to elucidate the dependence upon the band gap of A_n/A_e (the ratio of the cross-sectional areas for the nonellipsoidal and ellipsoidal models of the Fermi surface), we have calculated this ratio for various values of η/E_g. We have assumed $\kappa_1^2/\kappa_2^2=0.01$. The results are given in Table III(a). Note that the deviation from ellipsoidal behavior is not strongly dependent upon the value of η/E_g, and is significant only for magnetic field orientations within a few degrees of the binary axis. This is a consequence of the fact that $\kappa_1^2/\kappa_2^2\ll1$. We have, therefore, repeated the calculation for the larger value $\kappa_1^2/\kappa_2^2=0.047$ which arises from our ellipsoidal fit. The results are given in Table III(b). If, indeed, our large experimental value of the fundamental binary period P_1 is a consequence of the deviation of the Fermi surface from ellipsoidal shape, this choice of κ_1^2/κ_2^2 is unrealistically high, and will give too small a value of A_n/A_e, i.e., too large a correction. The correction based on the Cohen theory is thus too small *a fortiori* to produce a good fit to our data. Further investigation will be required to resolve the discrepancy, which may be due (a) to an undetected systematic error in the deviation of the periods from the data, or (b) to difficulties, as yet not clearly understood, in the interpretation of the Shubnikov–de Haas effect,[1] or (c) to the necessity of considering higher order terms in the Cohen model. If (a) is the case (i.e., the misfit in the region $0°\lesssim|\psi|\lesssim15°$ is not real), the ellipsoidal model gives quite a good fit to the data, again in disagreement with the very sharp departure from ellipticity near the binary predicted by the Cohen model (see Table III).

We may use the values $E_g=15$ meV and $\eta=30$ meV to calculate[18] n_e', the corrected light-electron concentration; with $\zeta_e=19.1$ meV we obtain $n_e'=1.1\times10^{17}$ cm^{-3}-ellipsoid^{-1}. The scatter in the points, and the

TABLE III. A_n/A_e as a function of ψ and η/E_g.

η/E_g \ ψ	90°	85°	75°	60°
		(a) $\kappa_1^2/\kappa_2^2=0.01$		
0.5	0.84	1.00	1.00	1.00
1.0	0.75	0.86	0.99	1.00
1.25	0.70	0.83	0.99	1.00
1.70	0.60	1.00	1.00	1.00
2.0	0.62	1.00	1.00	1.00
		(b) $\kappa_1^2/\kappa_2^2=0.047$		
1.25	0.70	0.80	1.00	1.00
2.0	0.62	0.71	1.00	1.00

[16] It may be argued that our large value of κ_1^2/κ_2^2 is evidence of an appreciable crystal misalignment. We can rule this out on the basis of (a) the agreement of our observed light-hole anisotropy with earlier results, and (b) the simplicity of our binary and bisectrix oscillations. The oscillations become complicated at very small angular displacements from the principal axes.
[17] M. H. Cohen, Phys. Rev. **121**, 387 (1961).
[18] D. Weiner, Phys. Rev. **125**, 1226 (1962).
[19] R. N. Brown, J. R. Mavroides, and B. Lax (to be published).

uncertainty in the analysis due to the nonellipsoidal shape of the Fermi surface, make it unprofitable to attempt to estimate ζ_e more closely for purposes of comparison with other results. We will see that a more enlightening discussion of the Fermi energies of the various carriers can be made on the basis of a study of the light-hole periods.

The Light-Hole Periods

The periods denoted in Fig. 3 by full triangles are attributed to the light holes. In paper I, the light-hole periods were seen only in a region within 15° of the trigonal axis. In this experiment, we have observed them throughout the range of magnetic field orientation. The periods fit very well to an ellipsoid of revolution with an axial ratio $\kappa_3^2/\kappa_1^2=3.55$. This value agrees within 5% with the results of Brandt[20] and of Galt *et al.*[13]

The error in determining the anisotropy ratio is due principally to uncertainty in the value of the light-hole periods near the bisectrix axis. In this region there are several competing periods, and there are errors due to beating effects. The trigonal period is $P_{h3}^{\rm II}=(1.42\pm0.04)\times10^{-5}$ G^{-1}; the accuracy is good due to the dominance of the light-hole periods near the trigonal axis. This value of $P_{h3}^{\rm II}$ yields $\kappa_3^2=22.8$ meV. If we assume the areal ratio given by Brandt *et al.*, $A_{12}/A_{23}=3.74$, we obtain $\kappa_1^2=1.65$ meV, and $n_h=3.92\times10^{17}$ cm^{-3}-ellipsoid^{-1}.

We may compare $P_{h3}^{\rm II}$ with the value obtained in paper I, $P_{h3}^{\rm I}=(1.54\pm0.02)\times10^{-5}$ G^{-1}, and thus obtain the shift in the Fermi level. The decrease in period is $\Delta P_h=-7.8\%\pm4\%$. As we have estimated the Fermi level $\zeta_h^{\rm I}$ to be 11.1 meV, we now have $\zeta_h^{\rm II}=12.0$ meV as the most probable value, and the absolute shift in the Fermi level is $\Delta E_F=(-0.9\pm0.4_5)$ meV. This value of ΔE_F is consistent with a difference in net impurity content between the two sets of samples of the order of one part per million. The proportional shift in the light-electron period, $\Delta P_e=+4.5\%$, is too small to have been observed.

The Heavy-Electron Periods

In paper I, we observed a set of isotropic heavy carriers of small Fermi energy and of unknown sign, with $P^{\rm I}=0.72\times10^{-5}$ G^{-1}, or $\kappa_{\rm I}^2=3.18$ meV. Here we observe an isotropic set of periods with $P^{\rm II}=1.23\times10^{-5}$ G^{-1}, from which we obtain $\kappa_{\rm II}^2=1.86$ meV, and $n^{\rm II}=1.29\times10^{17}$ cm^{-3}-ellipsoid^{-1}. These periods are denoted in Fig. 3 by open triangles to which we have fitted the dot-dash line. Only three periods assignable to this set are observed in the X–Y plane; these are denoted by dotted open triangles in order to emphasize the uncertainty inherent in assigning scattered points to a piece of Fermi surface. If this isotropic set of oscillations is attributable to the heavy carriers observed in paper I, the carriers must be electrons. This follows from the fact that their period is larger in the present work than in that of paper I, while that of the light holes is smaller. We will hence forth refer to these carriers with the subscript E.

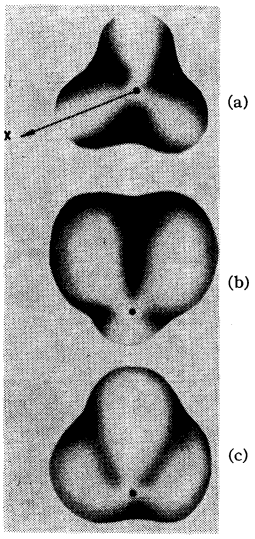

FIG. 4. The simplest possible form of the heavy-hole Fermi surface. The trigonal axis of the trefolioid must be parallel to that of the crystal. The maximum equatorial radii must be parallel to the binary axes of the crystal. (a) View from a direction in the X–Z plane. Trigonal axis shown as a dot. (b) View from a direction in the Y–Z plane. The surface has been rotated 60° about the trigonal axis, relative to (a). Trigonal axis shown as a dot. (c) View along trigonal axis. The arrow depicts a binary axis.

It is easy to show that

$$\zeta_E^{\rm I}=P_E^{\rm II}|\Delta\zeta|/\Delta P_E, \tag{2a}$$

$$\zeta_E^{\rm II}=P_E^{\rm I}|\Delta\zeta|/\Delta P_E, \tag{2b}$$

and

$$m_E^*=(e\hbar/m_0c)(\Delta P_E/|\Delta\zeta|)(P_E^{\rm I}P_E^{\rm II})^{-1}; \tag{2c}$$

here, $\Delta P_E=P_E^{\rm II}-P_E^{\rm I}$. From these expressions we obtain the values $\zeta_E^{\rm I}=2.17$ meV, $\zeta_E^{\rm II}=1.27$ meV, and $m_E^*=0.74$.

The Heavy-Hole Periods

We have observed two more classes of periods. One class is composed of scattered values, mostly very small. We are unable to account for these; they are denoted by small dots in Fig. 3. It is probable that at least some of them are spurious periods produced by beating. This is particularly likely for periods smaller than $\approx0.15\times10^{-5}$ G^{-1}.

The class of periods observed in the X–Y plane and denoted by squares in Fig. 3 appears to arise from a new piece of Fermi surface. The dot-dot-dash line has been sketched in as a rough fit to the periods. The binary period is approximately 0.5×10^{-5} G^{-1} and the bisectrix period approximately 0.8×10^{-5} G^{-1}. The accuracy of the points is approximately ±10%. No periods of this class are observed in the Y–Z plane.

We assert that this piece of Fermi surface contains the second set of heavy carriers—holes—required to satisfy electrical neutrality. The simplest possible form of this heavy-hole Fermi surface consistent with the

[20] N. B. Brandt, Soviet Phys.—JETP **11**, 975 (1960).

data is a trefolioid,[21] i.e., the figure depicted in Fig. 4. As we have no data for this surface in the Y–Z plane, we are unable to say whether it is a spherical or an ellipsoidal trefolioid, i.e., whether the maximum equatorial radius is or is not equal to the polar radius. It is reasonable, however, to assume that the heavy-hole surface, like the heavy-electron surface, is not highly anisotropic. We will therefore estimate the mean period to be $P_H^*=0.6\times10^{-5}$ G^{-1}. This yields a mean $\kappa_H{}^2=3.8$ meV and $n_H=1.7\times10^{17}$ cm^{-3}-ellipsoid^{-1}.[22] We defer estimates of m_H and ζ_H until we have considered the complete Fermi surface.

The Complete Fermi Surface

At this point, a knowledge of N_E/N_H (where N_E and N_H are the total concentrations of the heavy electrons and heavy holes, respectively) and the total carrier specific heat γ would lead directly to a set of diophantine equations from which we could extract the Fermi surface multiplicities q_E and q_H, and the heavy-hole Fermi energy and mean effective mass ζ_H and m_H^*. Unfortunately, N_E/N_H is not known; a shift in Fermi level, from the intrinsic value, of considerably less than 1 meV would suffice to make it impossible to determine q_E and q_H.

We may nonetheless set limits by means of the partial carrier specific heat

$$\gamma'=\tfrac{1}{2}\pi^2k^2[N_E/\zeta_E+N_H/\zeta_H]. \qquad (3)$$

If we adopt Kalinkina and Strelkov's value[23] of γ, corrected for the nuclear quadrupolar contribution,[1] it can be shown that $\gamma'=17.0\times10^{12}$ eV-deg^{-2}-cm^{-3}. Phillips's value[24] of γ yields $\gamma'=4.6\times10^{12}$ eV-deg^{-2}-cm^{-3}.[25] As each ellipsoid of heavy electrons contributes $\gamma_E{}^{\mathrm{II}}=3.71\times10^{12}$ eV-deg^{-2}-cm^{-3} (for Bi III and IV), or $\gamma_E{}^{\mathrm{I}}=4.85\times10^{12}$ eV-deg^{-2}-cm^{-3} (for Bi Ia, Ib, and II), it appears unlikely that our results can be reconciled with Phillips's value of γ. Even if we chose $q_E=1$, $q_H=1$, we would be forced to assign an unrealistically small effective mass to the heavy holes. We note that such a small effective mass has not been observed in cyclotron resonance experiments. The larger value of γ' is consistent with the set of parameters $N_E\approx N_H$, $q_E\approx3$, $q_H\approx2$, $\zeta_E\approx2$ meV, $\zeta_H\approx1$–2 meV, $m_E^*\approx0.7$, $m_H^*\approx1$, $N_{\mathrm{tot}}\approx15\times10^{17}$ cm^{-3}, but these must be regarded as very rough values. Note that the specific heat is not a sensitive indicator of sample purity (i.e., Fermi level) once the sample is pure enough so that all four sets of free carriers exist, since a decrease in one of the terms in brackets in Eq. (3) is approximately compensated for by an increase in the other. If our estimates are correct, we would expect the heavy-hole periods to have been approximately equal to the heavy-electron periods in paper I; this may be why two separate heavy carrier surfaces were not observed in our earlier work.

[21] We coin the word "trefolioid" for a geometric solid whose equatorial section is a trefoil by analogy with "ellipsoid," a solid whose equatorial section is an ellipse.

[22] The unit "cm^{-3}-ellipsoid^{-1}" is somewhat inappropriate here. We retain it nonetheless for the sake of consistency, since there is little chance of confusion.

[23] I. N. Kalinkina and P. G. Strelkov, Soviet Phys.—JETP **7**, 426 (1958).

[24] N. E. Phillips, Phys. Rev. **118**, 644 (1960).

[25] These values of γ' differ slightly from those given in Table V of reference 1. The small correction is the result of adopting the value of E_g given by Brown *et al.* (reference 19); this reduces the light-electron specific heat.

V. SUMMARY AND CONCLUSIONS

We have observed the differential Shubnikov–de Haas oscillations in a set of bismuth samples prepared by Zitter.[2] We have found the spin splitting of the light-electron Landau levels to be in agreement with the results of Boyle *et al.*,[3] and have extended the observations to magnetic field orientations along the bisectrix axis. We have observed departure of the light-electron Fermi surfaces from ellipsoidal form, and compared the results with the predictions of the Cohen model[17] and the results of Weiner[18] and of Brown *et al.*[19]

From the difference between the accurately measurable light-hole periods in this and in previous[1] work, we have been able to deduce the Fermi level shift, and to ascertain that the heavy carriers detected in both experiments are electrons; we have evaluated their Fermi energy and effective mass.

We have observed a new set of oscillations which we attribute to a heavy-hole band of trefolioid form. Due to the very small Fermi energies of this band and the heavy-electron band, we can make only a rough estimate of the heavy-hole Fermi energy and effective mass. It will be necessary to make measurements on samples of bismuth which are purer by an order of magnitude (impurity content 0.1 part per million or less) in order to evaluate these parameters accurately by quantum oscillation techniques.

ACKNOWLEDGMENTS

The author thanks Dr. R. Baron, Dr. T. Berlincourt, Professor M. H. Cohen, and Dr. D. Weiner for informative discussions of certain aspects of this problem; Mrs. M. Price for performing a part of the calculations; and the Institute for the Study of Metals of the University of Chicago for the use of their experimental facilities and for the loan of Zitter's samples.

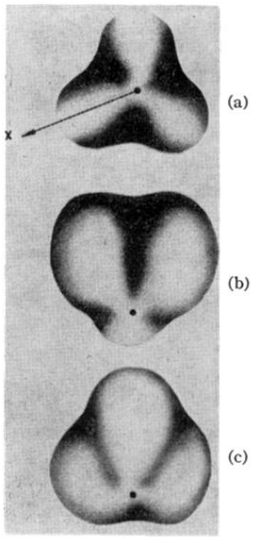

FIG. 4. The simplest possible form of the heavy-hole Fermi surface. The trigonal axis of the trefolioid must be parallel to that of the crystal. The maximum equatorial radii must be parallel to the binary axes of the crystal. (a) View from a direction in the X–Z plane. Trigonal axis shown as a dot. (b) View from a direction in the Y–Z plane. The surface has been rotated 60° about the trigonal axis, relative to (a). Trigonal axis shown as a dot. (c) View along trigonal axis. The arrow depicts a binary axis.